SCIENCE CHINA
Information Sciences

• **Supplementary File** •

MMSE Channel Estimation for Two-Port Demodulation Reference Signals in New Radio

Dejin KONG[1], Xiang-Gen XIA[2], Pei LIU[3*] & Qibiao ZHU[4]

[1]*School of Electronic and Electrical Engineering, Wuhan Textile University, Wuhan* 430200*, China;*
[2]*Department of Electrical and Computer Engineering, University of Delaware, Newark, DE* 19716*, USA;*
[3]*School of Information Engineering, Wuhan University of Technology, Wuhan* 430070*, China;*
[4]*School of Information Engineering, Nanchang University, Nanchang* 330031*, China*

Appendix A DFT-based Channel Estimation

The DFT-based scheme is briefly presented to achieve the channel estimation of two-port DMRS. Firstly, a P-point inverse DFT (IDFT) operation is performed on $\hat{\mathbf{h}}$, and it is obtained as

$$\hat{\underline{\mathbf{h}}} = \mathbf{F}\hat{\mathbf{h}} = \underline{\mathbf{h}}_{1r} + \underline{\mathbf{h}}_{2r}\left(\frac{P}{2}\right) + \boldsymbol{\xi}_r, \tag{A1}$$

where $\mathbf{F}$ is the IDFT matrix with dimension of $P \times P$, whose element at the position (p, q) is $\frac{1}{\sqrt{P}} e^{j2\pi \frac{pq}{P}}$, and $\boldsymbol{\xi}_r = \mathbf{F}\mathbf{X}^{-1}\boldsymbol{\eta}_r$. Also, $\underline{\mathbf{h}}_{tr}$ is the channel impulse response between the tth transmitting antenna and the rth receiving antenna, and $\underline{\mathbf{h}}_{2r}\left(\frac{P}{2}\right)$ is a cyclic shift vector of $\underline{\mathbf{h}}_{2r}$ with a shift $\frac{P}{2}$. Note that, the number of subcarriers in OFDM should be at least twice larger than the channel length.

From (A1), it can be observed that, the channel impulse responses $\underline{\mathbf{h}}_{1r}$ and $\underline{\mathbf{h}}_{2r}$ are separated by $\frac{P}{2}$ in the time domain as shown in Figure A1, and the time-domain channel estimation can be performed by the following function,

$$g(p) = \begin{cases} 1, \ 0 \leqslant p < \frac{P}{2} - 1, \\ \\ 0, \ \frac{P}{2} \leqslant p < P - 1, \end{cases} \tag{A2}$$

Denote a $P \times P$ diagonal matrix $\mathbf{G}$ with the diagonal element $g(p)$. Then, the channel estimation of $\underline{\mathbf{h}}_{1r}$ can be obtained as

$$\hat{\underline{\mathbf{h}}}_{1r} = \mathbf{G}\hat{\underline{\mathbf{h}}}. \tag{A3}$$

Then, the channel frequency responses can be obtained by a P-point DFT operation

$$\hat{\mathbf{h}}_{1r}^{\mathrm{DFT}} = \mathbf{G}\hat{\underline{\mathbf{h}}}_{1r}. \tag{A4}$$

As for $\mathbf{h}_{2r}$, the channel estimation can be performed by the same principle.

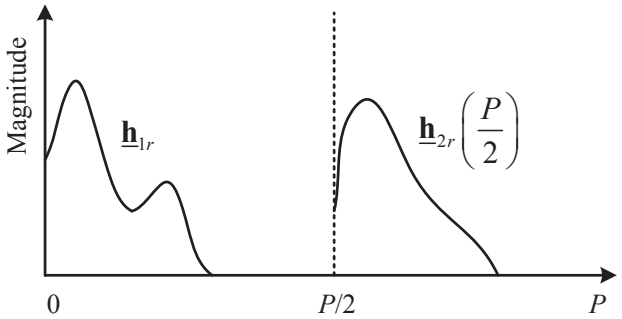

Figure A1 Separation of channels in the DFT-based channel estimation.

* Corresponding author (email: pei.liu@ieee.org)

Appendix B OCC-based MMSE

It is noted that, when $\Delta_{\rm cs} = P/2$ with an even number P for simplicity, the two DMRS ports, x_{2p}, x_{2p+1} for the first port and x_{2p}, $-x_{2p+1}$ for the second port with $p = 0, 1, \cdots, P/2-1$, can be separated by the orthogonal cover code (OCC), i.e., $[1, 1]$ and $[1, -1]$. In this subsection, the OCC-based MMSE channel estimation scheme is presented for the two DMRS ports.

Firstly, the channel estimation model can be obtained

$$\begin{cases} y^r_{2p}/x_{2p} = h^{1r}_{2p} + h^{2r}_{2p} + \eta^r_{2p}/x_{2p}, \\ \\ y^r_{2p+1}/x_{2p+1} = h^{1r}_{2p+1} - h^{2r}_{2p+1} + \eta^r_{2p+1}/x_{2p+1}, \quad p = 0, 1, \cdots, P/2-1. \end{cases} \tag{B1}$$

Note that, x_p has transmitting power of 1, therefore, noise η^r_p/x_p satisfies the Gaussian distribution with mean 0 and σ^2.

Assume that channel frequency responses, h^{tr}_{2p} and h^{tr}_{2p+1} are equal, i.e., $h^{tr}_{2p} = h^{tr}_{2p+1}$. Then, equation (B1) can be rewritten as

$$\begin{cases} y^r_{2p}/x_{2p} = h^{1r}_{2p} + h^{2r}_{2p} + \eta^r_{2p}/x_{2p}, \\ \\ y^r_{2p+1}/x_{2p+1} = h^{1r}_{2p} - h^{2r}_{2p} + \eta^r_{2p+1}/x_{2p+1}, \quad p = 0, 1, \cdots, P/2-1. \end{cases} \tag{B2}$$

Denote $\bar{y}^r_p = y^r_p/x_p$ and $\bar{\eta}^r_p = \eta^r_p/x_p$. Then, each user can perform the channel estimation independently as

$$\begin{cases} \hat{h}^{1r}_{2p} = \frac{\bar{y}^r_{2p} + \bar{y}^r_{2p+1}}{2} = h^{1r}_{2p} + \frac{\bar{\eta}^r_{2p} + \bar{\eta}^r_{2p+1}}{2}, \\ \\ \hat{h}^{2r}_{2p} = \frac{\bar{y}^r_{2p} - \bar{y}^r_{2p+1}}{2} = h^{2r}_{2p} + \frac{\bar{\eta}^r_{2p} - \bar{\eta}^r_{2p+1}}{2}, \quad p = 0, 1, \cdots, P/2-1. \end{cases} \tag{B3}$$

Then, the channel estimation can be improved by the MMSE criteria, which can be obtained as

$$\hat{\mathbf{h}}^{\text{OCC-MMSE}}_{tr} = \mathbf{R}_{tr} \left(\mathbf{R}_{tr} + \sigma^2 \mathbf{I}_{P/2} \right)^{-1} \hat{\mathbf{h}}_{tr}. \tag{B4}$$

where $\hat{\mathbf{h}}_{tr} = [\hat{h}^{tr}_0, \hat{h}^{tr}_2, \cdots, \hat{h}^{tr}_{P-2}]^T$. $\mathbf{R}_{tr}$ is the auto-covariances of $\mathbf{h}_{tr} = [h^{tr}_0, h^{tr}_2, \cdots, h^{tr}_{P-2}]^T$.

It is worthwhile noting that, the OCC-based MMSE is based the assumption $h^{tr}_{2p} = h^{tr}_{2p+1}$, which indicates a performance loss of channel estimation under highly frequency selective channels. Especially, for the two DMRS ports, the pilot symbols locate at every two subcarriers. Therefore, the channel frequency responses at m-th and $(m+2)$-th subcarriers are required to be equal in the classical OCC-based MMSE scheme.

Appendix C Simulation Result

Numerical simulations are carried out to show the validity of the proposed schemes in a 2×2 multiple-antenna OFDM system with $P = 120$ and $M = 2048$, in which the system sampling rate is 30.72MHz. In simulations, quadrature phase shift keying (QPSK) modulation and no channel coding scheme are considered. In addition, the length of cyclic prefix is 144 samples.

Figure C1 and Figure C2 depict the mean square error (MSE) and bit error ratio (BER) performances of the proposed P-MMSE and F-MMSE schemes, respectively. In simulations, the channel model with the exponential power delay profile are adopted. For comparison, we also give the performances of the classical DFT-based scheme and the OCC-based MMSE scheme. From simulation results, the proposed P-MMSE and F-MMSE schemes exhibit large gains in terms of MSE and BER compared with the classical DFT-based scheme, since the classical DFT-based scheme does not require the priori knowledge of channel covariance matrix. It is also observed that, compared with the proposed P-MMSE and F-MMSE schemes, the classical OCC-based MMSE can achieve similar MSE and BER performances at low SNR region and suffers from obvious loss at high SNR region. The reason is that the classical OCC-based MMSE is based on the assumption that the channel frequency responses at adjacent subcarrier are equal, which indicates performance loss under high frequency selective channels. Note that, pilot symbols of the two DMRS ports locate at every two subcarriers, therefore, the channel frequency responses at m-th and $(m+2)$-th subcarriers are required to be equal in the classical OCC-based MMSE scheme. On the other hand, the proposed F-MMSE scheme can achieve the optimal channel estimation performance, with the full priori knowledge of both DMRS ports, i.e., $\mathbf{R}_{1r}$ and $\mathbf{R}_{2r}$. When the two DMRS ports are assigned to two different users, the full priori knowledge is not easy to obtain for one user. The proposed P-MMSE only requires the priori knowledge of one port and can achieve the similar performance compared with the proposed F-MMSE, despite the large difference of the attenuation factors of exponential power delay profiles.

To evaluate the proposed schemes under more practical channel models, tapped delay line (TDL) models [1] released by 3GPP are also used in simulations. Note that, the two DMRS ports are assigned to different channel models. Specifically, the first DMRS port is with TDL-A and the second DMRS port is with TDL-C, in which TDL-A and TDL-C exhibit different delay spreads and power delay profiles [1]. Figure C3 shows BER comparison of the proposed P-MMSE scheme and F-MMSE scheme under the TDL channels. From simulation results, the proposed P-MMSE achieves the similar BER performance compared with the optimal F-MMSE, which validates the effectiveness of the proposed P-MMSE scheme.

When only one of the two DMRS ports is used, the 2×2 multiple-antenna OFDM system becomes a 1×2 multiple-antenna system. However, for one user with the first DMRS port, it is difficult to obtain the priori knowledge on whether another DMRS port is used or not. Figure C4 shows the BER performance of the proposed P-MMSE scheme under the TDL channels when only one of the two DMRS ports is used. For comparison, the performance of the optimal MMSE is also given. From simulation results, the proposed P-MMSE achieves a similar BER performance compared with the optimal MMSE.

Then, the first DMRS port is with the TDL-C channel and the second DMRS port is with the channel with equal-power power delay profiles and maximum channel delay spread $9.65860\mu s$. Figure C5 shows BER comparison of the proposed P-MMSE scheme and F-MMSE scheme under the TDL channel and the channel with equal-power delay profiles. From simulation results, the proposed P-MMSE achieves the similar BER performance compared with the optimal F-MMSE, which validates the effectiveness of the proposed P-MMSE scheme. Besides, the classical OCC-based MMSE suffers from obvious performance loss. The reason is that the classical OCC-based MMSE is based on the assumption that the channel frequency responses at adjacent subcarrier are equal, which is not satisfied well under the high frequency selective channels.

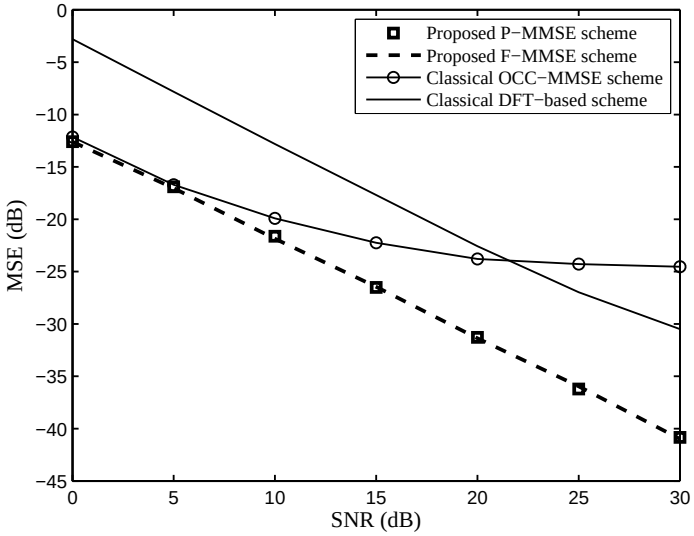

Figure C1 MSE comparison of the proposed P-MMSE scheme, the proposed F-MMSE scheme, and the classical DFT-based scheme under channels with exponential power delay profiles.

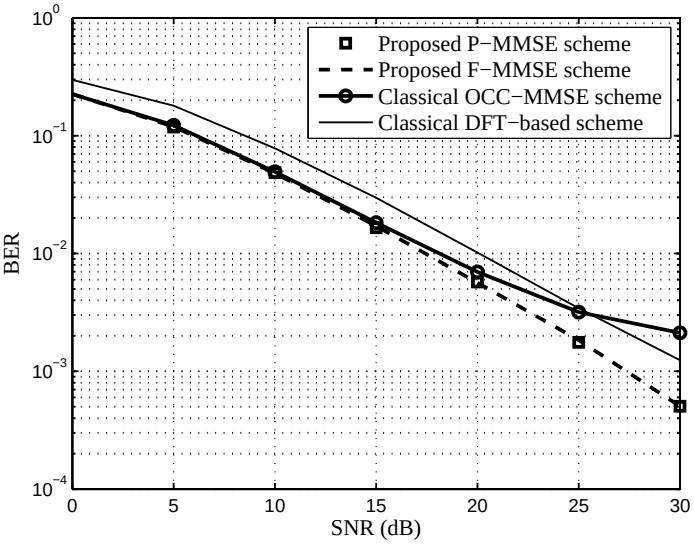

Figure C2 BER comparison of the proposed P-MMSE scheme, the proposed F-MMSE scheme, and the classical DFT-based scheme under channels with exponential power delay profiles.

References

1 3GPP. Technical specification group radio access network; study on channel model for frequencies from 0.5 to 100 GHz (Release 16). v16.1.0, TS 38.901, 2019. [Online]. Available: https://www.3gpp.org/ftp/Specs/archive/38_series/38.901/38901-g10.zip

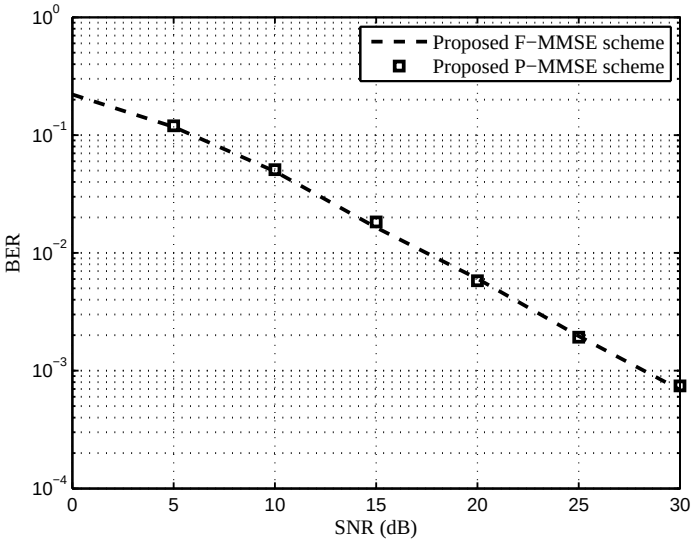

Figure C3 BER comparison of the proposed P-MMSE scheme and the proposed F-MMSE scheme, under the TDL channels.

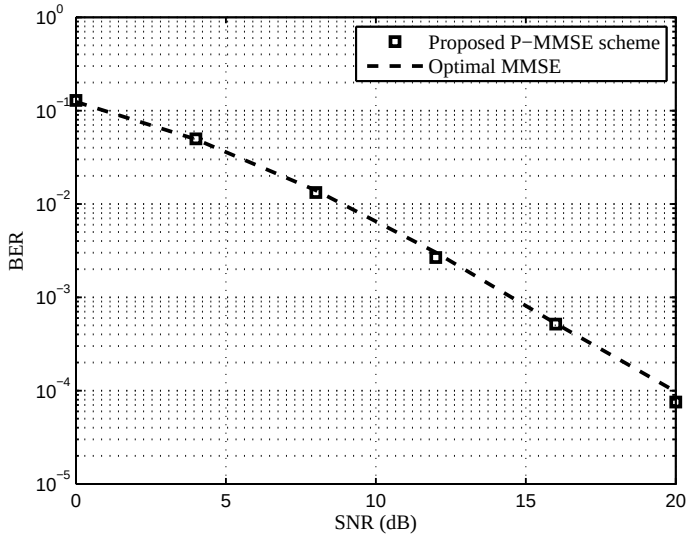

Figure C4 BER performance of the proposed P-MMSE scheme under the TDL channels when only one of the two DMRS ports is used.

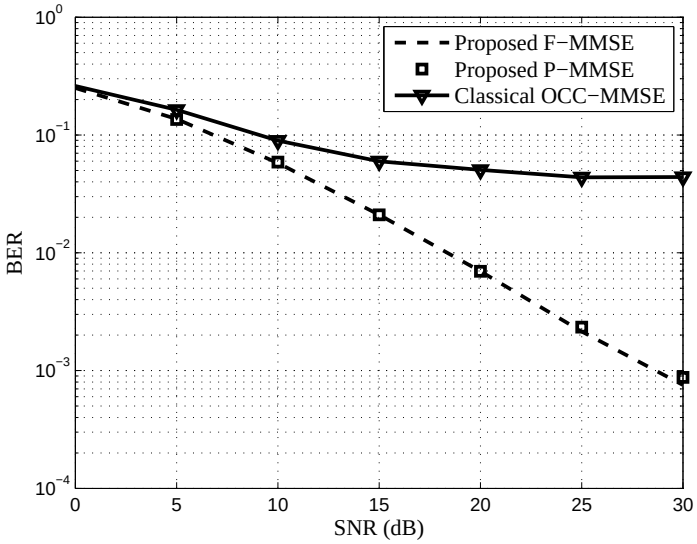

Figure C5 BER performance of the proposed P-MMSE scheme under TDL-C and the channel with equal-power delay profiles.